Steering bio-electro recycling of carbon dioxide towards target compounds through novel inoculation and feeding strategies

R. Blasco-Gómez [a], M. Romans-Casas [a], S. Bolognesi [a,b], E. Perona-Vico [c], J. Colprim [a], L. Bañeras [c], M.D. Balaguer [a], S. Puig [a,*]

[a] LEQUIA, Institute of the Environment, University of Girona, 69, Maria Aurèlia Capmany, Girona 17003, Spain
[b] Department of Civil Engineering and Architecture, University of Pavia, Via Adolfo Ferrata 1, Pavia 27100, Italy
[c] Group of Molecular Microbial Ecology, Institute of Aquatic Ecology, University of Girona, 40, Maria Aurèlia Capmany, Girona 17003, Spain

ARTICLE INFO

ABSTRACT

New strategies in inoculation and operation of bioelectrochemical systems were used to advance in the steering of bio-electro carbon dioxide (CO_2) recycling towards chemical compounds. First, the preparation of microbe coated biocathodes *ex-situ* with putative electroactive species with CO_2 as sole carbon source was assayed. Second, CO_2 feeding strategies for the operation of BES systems were explored to ensure enough reducing power during batch mode operation. The impact on the proposed changes on the product portfolio and production yields was assessed. The initial enrichment of a putative electroactive community on bare electrode surfaces was proven to be successful and led to a shortening of the start-up period of the system from days to hours. Moreover, the establishment of a new feeding procedure to favor the presence of elevated reducing power availability for cells triggered the production of longer carbon chain carboxylates (max. 0.99 $g_{butyrate}$ $m^{-2}_{electrode}$ d^{-1}) and alcohols (max. 0.83 $g_{ethanol}$ $m^{-2}_{electrode}$ d^{-1}) at early stages of experiment. This work complements the recent knowledge on the control of bioelectrochemical processes by the establishment of strategies to obtain target added-value compounds from CO_2.

1. Introduction

The production of chemicals and liquid fuels from waste gaseous streams using microbial electrochemical technologies (METs) has attracted an increasing attention. The capability of some microorganisms to act as biocatalyst for the reduction of CO_2 into commodity chemicals by means of renewable electricity is nowadays the base of a sustainable platform to mitigate global warming [1,2].

Acetate has been the main produced compound by most attempts aiming to convert CO_2 into building blocks. However, recent studies have demonstrated that C3-C6 compounds such as isopropanol, butyrate, butanol, caproate and hexanol may also be obtained through CO_2 bio-electro recycling [3–9]. Some authors pointed out the adjustment of operational parameters and novel reactor designs as plausible strategies to improve the selectivity towards those organics required to produce larger carbon compounds. For instance, setting high CO_2 loading rates (173 L d^{-1}) and high hydraulic retention times (14 days) during operation promoted an increased production and selectivity of butyrate and caproate [9]. Moreover, bioelectrochemical systems (BESs) operated

with tight pH control ($\approx$5) and low-buffered media led to an increase in chain elongation processes [8]. In relation to reactor design, the addition of an extra cathodic chamber in BESs opened the possibility to separate processes that require different operational parameters and improved the selectivity of uncoupled metabolic pathways [10].

In spite of the previous advances in process control, the economic feasibility of BES as a resource recovery technology is subjected to a better knowledge of how to better steer the process [11], i.e. increasing product titters and energy conversion yields. It is essential to choose the target compound based not only on the market opportunities and value but also on the requirements and conditions for its in-situ recovery [12]. Such tighter control should be accomplished by defining the operational parameters that would allow the operator to conduct the biological reactions towards the production of desired compounds (e.g. carboxylates or alcohols). pH, dissolved CO_2 and hydrogen partial pressure (pH_2) were reported as critical operational parameters to switch from acetogenesis to solventogenesis pathways in BESs [13]. A continuous monitoring of key-parameters during the bio-electro recycling of CO_2 and the whole operation is essential to improve the future product selectivity and overall competitiveness of METs.

Nomenclature

BES	Bioelectrochemical system
CA	Chronoamperometry
CE	Coulombic efficiency
CO_2	Carbon dioxide
cTAB	Cetyltrimethylammonium bromide
CV	Cyclic voltammetry
DNA	Deoxyribonucleic acid
FID	Flame ionization detector
GC	Gas chromatograph
H_2	Hydrogen
MET	Microbial electrochemical technology
OD	Optical density
OTUs	Operational taxonomic units
PCR	Polymerase chain reaction
rRNA	Ribosomal ribonucleic acid
SHE	Standard hydrogen electrode
TCD	Thermal conductivity detector

On the biological aspects of the technology, the formation of an effective and mature biofilm settled on the surface of the electrode that acts as biocatalyst is mandatory to obtain more complex molecules in a long-term operation [7]. High amounts of cells are indeed required to achieve high energy efficiencies. Therefore, new methodologies to reinforce the attachment of the electroactive microorganisms to the electrode surface must be established. At the same time, mature biofilms require higher and continuous reducing power available to allow the production of desired compounds.

The main objective of the present study was to give new insights into the bio-electro CO_2 recycling into short chain carboxylic acids, attempting to a tighter control of the entire process. First, a new inoculation protocol was established to develop an electroactive community on the electrode surface. Second, a novel CO_2 feeding strategy based on avoiding the flush out exceeding hydrogen during each feeding event was assessed to increase the available reducing power at favorable thermodynamic conditions throughout the entire process. In addition, the proposed strategy resulted in a non-invasive and friendly strategy from the point of view of the maintenance of the biofilm. Up to our knowledge, the proposed feeding strategy is unique in the framework of

bio-electro CO_2 recycling. So far, the studies consulted in the literature working with microbial electrosynthesis cells operated in batch used the same conventional feeding strategy. H_2 produced biotically or abiotically in the cathode during previous batches was completely flushed and therefore the initial stage of the subsequent batch lacked enough reducing power. The only studies found that described an alternative feeding operation were based on the continuous recirculation of the surplus CO_2 and its flow rate variation to improve the CO_2 utilization rate and enhance the gas–liquid mass transfer, respectively [14,15]. In such case, improving CO_2 availability to the biofilm by recirculating it from the gas-phase boosted the system performance by an increase of 44% in the acetate production. Alternatively, the feeding strategy proposed in this manuscript not only kept the not converted CO_2 remained in the system, but also the H_2 produced in previous batches.

2. Materials and methods

2.1. BES set-up

Two flat-plate BESs were set as duplicates and named Reactor 1 (R1) and Reactor 2 (R2) (Scheme: Fig. 1, Images: Figs. S1 and S2). The systems consisted of two methacrylate compartments of 185 mL each separated by a cation exchange membrane (CEM) (CMI-1875T, Membranes international, USA) of 82.7 cm^2 (4.4 cm width and 18.8 cm length).

The anode consisted of commercial carbon cloth (Thickness 490 μm; NuVant's ELAT, LT2400W, FuelCellsEtc, USA) with a working surface of 129 cm^2 (4.3 cm width and 15 cm length) that was connected to a graphite rod (0.45 cm diameter and 4.4 cm of length, Mersen Iberica, Spain). Carbon-based anodic electrodes were chosen over metal-based ones (i.e. Ti or Pt) to catalyze the water oxidation reaction due to its lower cost and less proneness to produce chlorine, which might inhibit the microbial activity in the biocathode. Carbon cloth has been previously used as anodic material for catalysing water oxidation [16,17]. A 129 cm^2 flat carbon cloth (working surface, like the anode) was used as cathode electrode connected to the power source through a stainless-steel wire. Systems were operated in a three-electrode configuration with a potentiostat (BioLogic, Model VSP, France), which controlled the cathode potential at − 0.8 V vs. SHE and monitored the current density. The biocathode was used as working electrode, the anode as counter electrode, and an Ag/AgCl electrode 0.197 V vs. SHE (sat. KCl, SE11-S Sensortechnik Meinsberg, Germany) placed in the cathode chamber was used as reference electrode.
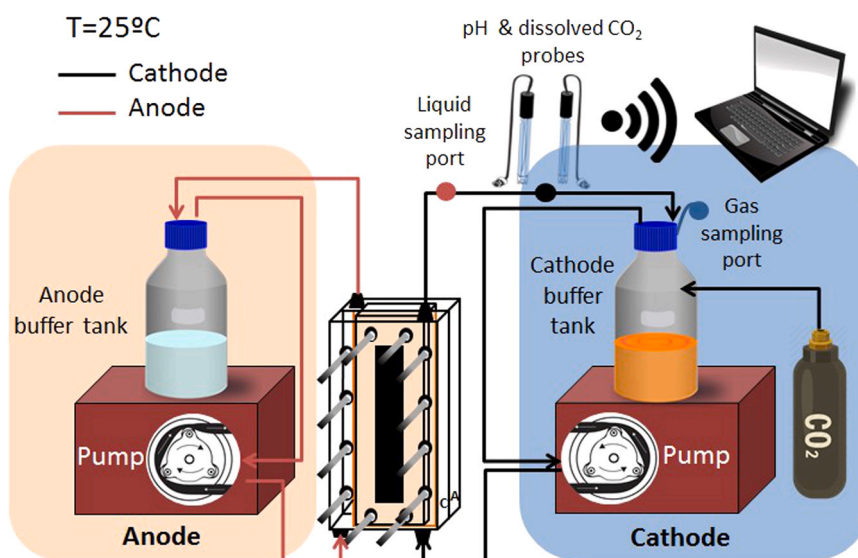

Fig. 1. Schematic representation of the flat-plate BES setup (reactors 1 and 2).

External buffer tanks were coupled to both anode and cathode chambers, respectively. The liquid was continuously recirculated at a constant flow rate of 4.5 L h^{-1} by two pumps (Watson-Marlow 323S, Watson-Marlow Fluid Technology Group, USA) to improve flow distribution and enhance mass transfer to increase the availability of substrate. The total volume of each compartment was 335 mL. 185 mL corresponded to the cathodic/anodic chamber and 50 mL to each buffer tank. Headspace volume of each buffer tank was 165 mL. Both BESs were operated at room temperature ($25 \pm 1\ °C$) and kept in the dark throughout the entire experiment.

Dissolved CO_2 and wireless pH probes were placed in the outlet of the cathodic chamber, within the recirculation flow circuit. Cathodic buffer tank housed ports for CO_2 feeding, and sampling the gas phase. The liquid samples were taken between the outlet of the cathodic chamber and the pH/dissolved CO_2 probes. Withdrawn sampling liquid was replaced with the same volume of freshly prepared medium saturated with CO_2.

2.2. Biocatalyst, growing conditions and transfer to BESs

Both cathode carbon cloths of R1 and R2 were initially enriched with potentially electroactive bacteria in a fermenter and progressively adapted to autotrophic conditions. The fermenter was inoculated with the isolate I-19 whose features were indicated elsewhere [13] and fed under autotrophic conditions with CO_2/H_2 (80:20% *v/v*, Praxair, Spain) gas mixture for 45 days. This gas mixture was chosen to previously adapt the microbes to the low-energetic environment expected in the cathodic chamber at the early stage of the experiment. The long incubation period foresaw a step-wise shift of the microbial community from heterotrophic to autotrophic metabolism. A characterization of the community in both the carbon cloth and the bulk liquid was carried out as well as, the quantification of the species present. After 45 days of operation, the bioelectrodes were placed in the cathodes of BES (Reactor 1 and Reactor 2) under an anaerobic chamber, filled with anaerobic fresh medium and, subsequently connected to the potentiostat. Thereby, the electron donor (H_2) was substituted with a carbon cloth colonized by electroactive bacteria that in-situ catalyzed the H_2 evolution reaction.

2.2.1. Electroactive microbe

Experiments were conducted with *Eubacterium* sp. I-19, an isolate that was obtained from sheep manure and exhibited equimolar production of ethanol and acetate in BES fed with CO_2 as the sole carbon source and operated at 25℃ [13,18]. Despite an axenic culture was used for inoculation, no sterile conditions were used in the rest of experiments performed. I-19 cultures were maintained in serum capped bottles under autotrophic conditions until late stationary phase (OD_{600} ~0.6) using a modified ATCC1754 PETC medium (Table S1). Medium was prepared anaerobically and pH was adjusted to 6. Cultures were flushed on a two to three day basis with syngas (32% CO, 32% H_2, 28% N_2 and 8% CO_2; *v/v*) for at least five minutes, and kept at an overpressure of 100 kPa at 37℃ [18]. Transfers to freshly prepared medium were performed at a 10–20% ratio for maintenance.

Previously to its inoculation in the flat-plate BESs (Section 2.2.4), I-19 cultures were transferred to organic (containing YE at 1.5 g/L) medium at 30 °C under anaerobic conditions fed periodically with CO_2:H_2 (80:20% *v/v*) (Praxair, Spain) as described in the following section (Section 2.2.3).

2.2.2. Preparation of bacterial coated biocathodes

In order to provide new insights in speeding up BES start-up time, carbon cloth cathodes were incubated in a fermentation chamber to promote formation of biofilms. The fermentation cell made of methacrylate and had a total volume of 410 mL (15 cm length, 10 cm width and 2.7 cm depth) (Fig. S3) and was connected to a buffer tank of 300 mL of total volume. A pump (Watson-Marlow 505 U, Watson-Marlow Fluid Technology Group, USA) was continuously recirculating medium at a constant rate of 7 L h^{-1}. The outlet was used to take samples. Carbon cloth pieces (Thickness 490 μm; NuVant's ELAT, LT2400W, FuelCell-sETc, USA) of 129 cm^2 (4.3 cm width and 15 cm length) were placed inside the fermenter and maintained separated using plastic spacers (Fig. S3). One of these carbon cloths was used to analyse the biological community.

The chamber was continuously flushed with pure N_2 gas (99.9%, Nippon gases, Spain) to avoid the presence of O_2. The cell was inoculated, filled with 500 mL of organic medium (Table S2) and subsequently inoculated with 200 mL of a Eubacterium I-19 early exponential culture adapted to CO_2:H_2 (80:20% *v/v*).

2.2.3. Operation of the fermentation cell

The gas and liquid phases were sampled twice a week right before feeding with gas. Gas samples were taken from the headspace of the buffer tank and collected in a 5 mL Vacutainer®. Liquid samples were taken directly from a sampling port located in the outlet of the fermenter cell.

After each sampling event the cell was opened in an anaerobic chamber and three samples of 0.25 cm^2 from the sacrificial carbon cloth were extracted to study the biofilm formation. The samples were taken from three different areas of the carbon cloth (both extremes and the middle; Fig. S4). 10 mL from the liquid phase were collected and centrifuged (Centrifuge 5702R, Eppendorf, Germany) at 4400 rpm under 4 °C for 20 min and supernatants were discarded. Both carbon cloth pieces and pellets were stored in the freezer at − 20 °C for further analysis. Withdrawn volume was replaced with modified ATCC1754 PETC medium whose pH was previously adjusted to 6 and flushed with N_2 (Praxair, Spain) to ensure the absence of O_2. Thus, reducing the presence of organic matter in the system. After that, the fermenter was placed in the original position and reconnected to the buffer tank. Afterwards, the system was fed with CO_2:H_2 (80:20% *v/v*) until saturation and the normal operation was re-established.

2.2.4. Transfer of the enriched electrodes to BES

After 45 days of operation, fermenter presented operational conditions comparable to BES (similar pH and autotrophy). A thin layer of biofilm was visible with the naked eye. Two of the carbon cloths were placed in the cathodic chambers of two flat-plate BES in anaerobic conditions using the anaerobic chamber. Half of the volume of the fermentation media was employed to inoculate each BES and both chambers (cathode and anode) were completely filled with fresh modified ATCC 1754 PETC medium saturated with pure CO_2 (99,95%, Praxair, Spain).

2.2.5. Start-up and operation

Both flat-plate BESs reactors were inoculated as described above and operated in batch-mode. Inorganic carbon in the form of CO_2 was used as the only carbon source, which was supplied every 2–3 days (Table 1) by feeding pure CO_2 (99.9%, Praxair, Spain). Two feeding strategies were followed to assess their impact in the compounds obtained and their production rates. First strategy followed was to bubble with CO_2 until saturation, whereas the second strategy consisted of feeding with CO_2 until an overpressure of 350–400 mbar was reached in the headspace without flushing remaining H_2 from the previous production

Table 1

Operational conditions of each batch during the experimental study. In the feeding strategy row, "S" corresponds to complete CO_2 saturation and "NS" means non-saturation CO_2 of the medium.

	Batch			
	1	**2**	**3**	**4**
Reactor 1 & 2 (days)	0–57	57–107	107–141	141–175
Feedings per week (n)	3	3	2	2
Feeding strategy	S	S	NS	NS

stage. The frequency chosen for feeding with CO_2 was higher (3 days) in the first two batches and lowered from the third batch onwards. Thereby, a pH range of 3.8–5.3 was maintained and enabled to monitor the switch of metabolic pathways within the biological community. A slightly higher pH was measured at the beginning of each batch, which corresponded to the initial pH of the fresh medium added (pH ≈ 6).

2.3. Chemical analysis

On-line CO_2 dissolved measurements in the liquid phase were carried out using a sensor (InPro®5000, Mettler-Toledo, USA). The data was continuously collected in a 2-channel transmitter (M800 Multi-Parameter transmitter, Mettler-Toledo, USA) that acted as datalogger. Both *on-line* pH and CO_2 dissolved measurements were taken at intervals of 5 min.

Gas samples of the tubular systems were collected with a glass syringe (500 μL Hamilton Samplelock Syringe, Hamilton, USA) and subsequently analysed in an Agilent 490 Micro GC (Agilent Technologies, USA) equipped with a Molsieve 5 Å and PoraPLOT U columns in parallel coupled to a thermal conductivity detector (TCD) detector.

The pressure of the gas phase in the headspace of the BES was continuously measured every 5 min using two pressure transducers (CirrusSense TDWLB Gen1, Transducer Direct, USA) that sent real-time information to an Apple Ipod (Ipod Touch 6th Gen, USA) that gathered the information through the Dataworks data app.

Conductivity was analysed at the end of each batch with an electric conductivity meter (EC-meter basic 30 +, Crison, Spain). Continuous pH measurements were carried out using two pH probes (IH40AT, Ionode, Australia) coupled to a wireless emitter (Bluebox-pH, Instrumentworks, Australia) that sent real-time data to an Apple Ipod (Ipod Touch 6th Gen, USA) which gathered the information through the Dataworks data app.

Carboxylic acids and alcohols present in the liquid phase were analysed every two or three days with an Agilent 7890A (Agilent Technologies, USA) GC equipped with a DB-FFAP column and a flame ionization detector (FID). Before the analyses, each sample was firstly acidified with ortho-phosphoric acid (85%, Scharlau, Spain) and subsequently crotonic acid (98%, Merck, Germany) was used as internal standard to ensure the results obtained.

The optical density (OD) of the catholyte was periodically measured to control the growth of the bulk microbial community with a spectrophotometer (CE 1021, 1000 Series, CECIL Instruments Ltd., UK) at a wavelength of 600 nm.

2.4. Analytical determinations and calculations

Two different potentiostats (SP-50 and VSP models, BioLogic, France) working in a three-electrode configuration controlled the voltage and fixed the cathode potential. The system was operated in chronoamperometry (CA) mode with a fixed potential of − 0.8 V vs. standard hydrogen electrode (SHE). Electrochemical-related parameters such as current signal, cell potential and power consumed were continuously monitored and registered once every 5 min. All the voltage values that appear throughout this manuscript are related to the SHE.

The calculation of the coulombic efficiency (CE) was based on the comparison of the energy consumed and the energy contained in the final compounds produced, which is the reason why is expressed in percentage (%). This equation was summarized by Patil and colleagues [19]. The CE was calculated using the following equation (Eq. (1)).

$$CE = \frac{F \cdot \Sigma_i M_{e,i} \cdot \Delta_{e,i}}{\int I \, dt} \cdot 100 \qquad (1)$$

Where F is the Faraday's constant; $M_{p,i}$ corresponds to the moles of product (i); $\Delta_{e,i}$ is the difference (in degree) of reduction between substrate and product (i.e. moles of electrons per mol of product); and $\int I \, dt$ is the integration of the current supplied over time.

H_2 concentrations in the whole system (gas + liquid phase) were calculated according to Henry's law of ideal gases compensated by temperature and total pressure values and using the following constants ($K_{H_2}^{\theta} = 7.8 \cdot 10^{-4}$ mol L^{-1} atm^{-1}, $T = 25$ °C).

Measured concentrations of organic acids and alcohols were transformed to mol C equivalents according to the corresponding mass weight. The moles produced of each compound were presented as function of time and normalized to total working volume.

Production rates were calculated as increments in concentration per unit between consecutive sampling points.

2.5. DNA extraction and microbial community structure determination

At the end of the operation (day 45) three samples from the carbon cloth (Fig. S4) and one bulk liquid were collected under anaerobic conditions. Pieces of carbon cloth electrode were taken directly using sterile forceps and scissors for biofilm measurements. 10 mL samples were centrifuged (4400 rpm, 15 min, 4 °C) and supernatants discarded for bulk measurements. Both electrode and pelleted cells were stored at − 20 °C until DNA extraction. DNA was extracted using a cetyl-trimethylammonium bromide (cTAB) based protocol [20]. The extracts were distributed in aliquots and stored at − 20 °C, and DNA concentration was measured using a Nanodrop™ 1000 spectrophotometer (Thermo Fisher Scientific, USA). Quality of DNA extracts for downstream molecular applications was checked after PCR detection of 16S rRNA using the universal bacterial primers 27F and 1492R.

The hypervariable V4 region of the 16S rRNA gene for all the samples was amplified using the primers 515F and 806R following the method described by Kozich and Schloss, which was adapted to produce dual-indexed Illumina compatible libraries in a single PCR step [21]. First, PCR was performed using fusion primers with target-specific portions [22], and Fluidigm CS oligos at their 5′ ends. Second, PCR targeting the CS oligos was used to add sequences necessary for Illumina sequencing and unique indexes. PCR products were normalized using Invitrogen SequalPrep DNA normalization plates and the pooled samples were sequenced using an Illumina MiSeq flow cell (v2) in a 500-cycle reagent kit (2×250bp paired-end reads). Finally, sequencing was done at the RTSF Core facilities at the Michigan State University USA (https://rtsf.natsci.msu.edu/).

Sequences were filtered for minimum length (> 250 nt) and maximum expected errors (< 0.25). Paired-end sequences were merged, quality filtered and clustered into OTUs (Operational Taxonomic Units) using USEARCH v9.1.13 [23]. They were clustered at the 97% identity using UCLUST [24], and checked for the presence of chimeras. OTUs containing only one sequence (singletons) were removed. The subsequent analyses were performed with Qiime v1.9.1 [25]. Representative OTU sequences were aligned using PyNAST with default parameters against Silva 132 release (April 2018). The same reference database was used to taxonomically classify the representative sequences using UCLUST. Direct BLASTn searches at the NCBI of selected sequences were used when poor identifications with the Silva database were obtained. Richness (Observed species and Chao1) and alpha diversity indices (Shannon and PhyloDiversity) indicators were calculated.

3. Results and discussion

3.1. Development of a resilient electroactive biofilm

Measurements right after the inoculation of the fermenter cell showed that carboxylates and alcohols were introduced together with the inoculum at the beginning of the experiment. In addition, the presence of yeast extract in the fresh medium triggered biofilm development throughout a transition from fermentation to carbon assimilation (Fig. 2). On the first stage, 0–28 days, simple organic products, mainly ethanol and acetate, were produced probably as a result of the
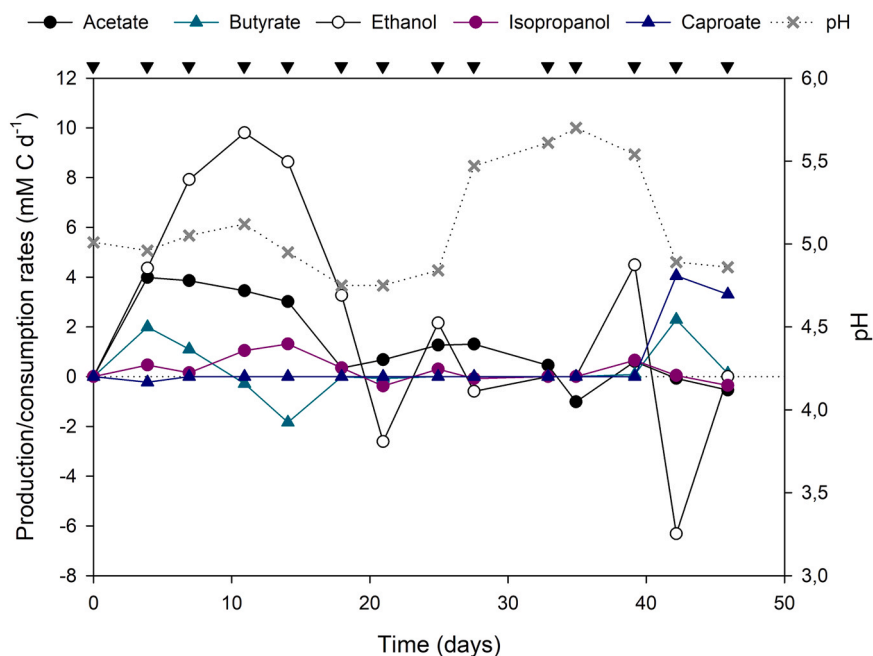
Fig. 2. Evolution of pH, carboxylates and alcohols in the fermenting medium during the fermentation cell operation. Black inverted triangles on the top of the figure indicate feeding events with CO_2:H_2 (80:20% *v/v*). The shift from heterotrophic to autotrophic was set at day 28.

fermentation of organic matter present in the medium composition (yeast extract and sugars; Table S2). Acetate and ethanol reached concentrations of 43.3 and 67.7 mM C, respectively. The microbial community averaged productions of 3.6 mM C d^{-1} of acetate and 7.7 mM C d^{-1} of ethanol in the first 14 days of operation where heterotrophic metabolism prevailed over autotrophic. During this period, pH decreased to 4.75 due to the accumulation of acids in the medium and was manually adjusted to 5.5 by replacing the liquid phase with strictly inorganic medium. After that, autotrophic fixation of CO_2 started and therefore resumed carboxylates and solvent production. Fermenting activity decreased between days 15 and 35 due to both depletion of organic matter and low pH values. After the day 35, an ethanol production peak could be observed (4.5 mM C d^{-1}) that was followed by its consumption leading to the formation of butyrate (2.3 mM C d^{-1}) and caproate (4 mM C d^{-1}), which can be very likely explained by reverse β-oxidation route. During this time, acetate concentration remained at low values (<5 mM C), which means that the decrease of pH value under 5 is explained by the accumulation of caproic and butyric acid. The maintenance of biological activity under the rather low pH values might only happen under the sub-optimal working temperature (25 °C), which helped to prevent acid crash by reducing acids accumulation rate inside the cell [26].

3.2. Analysis of the biological community structure

Three samples from the three different regions (Sections 1, 2 and 3; Fig. S4) along the carbon cloth (129 cm^2) and one sample of the bulk liquid in the last day of operation (day 45) were characterized to study the microbial community. A total of 236.958 high quality sequences were identified and diversity coverage was higher than 95%. The number of operational taxonomic units (OTUs) identified (considered as an index of observed diversity) were 60 and 45 accounting the three carbon cloth samples together and the bulk liquid, respectively. In addition, microbial diversity was calculated through the Shannon's index (H′) and resulted in 3.2 for the carbon cloth samples and 2.9 for the bulk liquid. Taxonomic identification of the sequences determined that the major phyla presented in both biofilm and bulk liquid communities were *Firmicutes*, *Actinobacteria* and *Proteobacteria*.

Interestingly, phyla relative abundances varied along the carbon cloth (Fig. S5), which might be explained by differences in nutrient availability and physical-chemical conditions inside the fermenter. Region CC1 of carbon cloth had a higher availability of nutrients due to its proximity to the gas inlet and a higher CO_2 availability and turbulence due to the fermenter's design. Compared to other carbon cloth sampling points the predominant phylum (*Firmicutes*) had a higher relative abundance (75.2% compared to 49.6% and 50.5% of CC2 and CC3, respectively). Samples from CC2 and CC3 had microbial community structures similar to the planktonic (bulk liquid) one. Even though, *Proteobacteria* was more abundant in the bulk liquid (22.3%) compared to the carbon cloth (4.69%, 6.27% and 7.71%, respectively).

At genus level, substantial differences were observed between sampling points (Fig. 3). Dominant genera in all samples were *Cellulomonas* and *Clostridium*. Although the fermenter was inoculated with an enriched culture of the isolate I-19 (*Eubacterium* genus in Fig. 3), the strain only represents the 19–5% of the total sequences identified in the carbon cloth. Further determinations using BLASTn comparisons confirmed the presence of *Eubacterium limosum* strain JMC 6421 (comparable to isolate I-19) with a 100% of identity. This strain was more abundant in the biofilm at the closest point of the inlet, where the carbon source (CO_2 dissolved) availability was higher.

Eubacterium spp. is known for its capability to produce fuels and chemicals [27], although its absence in the catholyte suggested that CO_2 utilization was ubiquitous in the fermenter by other species (e.g. *Clostridium*) to produce more complex molecules such as butyrate and caproate [28,29]. *Enterococcus* (highly abundant at region CC1) has been related to extracellular electron transfer and pyruvate production [30].

Together with *Cellulomonas* and *Clostridium*, *Pseudomonas*, *Burkholderia* and *Citrobacter* were the most representative genera at bulk liquid sample (8.5%, 8.1% and 5.4% relative abundances, respectively). *Pseudomonas* was described before as a genus with high capability of electron exchange, very active in syntrophic interactions [31], and was also linked with CO_2 bio-electro recycling [32,33]. The presence of *Burkholderia* might be ensuring anoxic conditions due to its activity as oxygen scavenger [34,35]. Moreover, this genus is known to be electroactive and able to produce short chain carboxylic acids under microaerophilic conditions [36]. *Citrobacter* is electroactive and able to
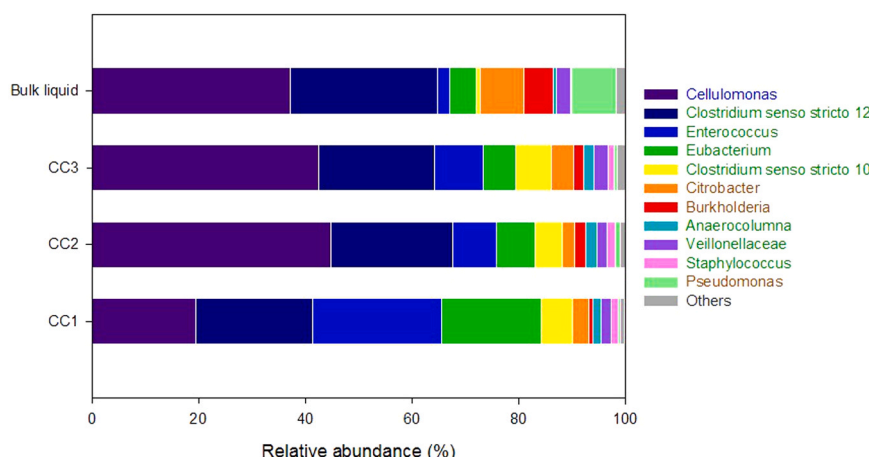
Fig. 3. Relative abundances of the observed genera in the microbial communities. Legend font colors are referred to the different phyla identified: *Firmicutes* (green), *Actinobacteria* (blue) and *Proteobacteria* (brown). All the genera with relative abundances below 1% were classified as others. (For interpretation of the references to color in this figure legend, the reader is referred to the web version of this article.)

produce propanediol [37].

3.3. Overall performance of BES and the effect of the new feeding strategy on the product spectrum

Two of the carbon cloth electrodes enriched with microorganisms suitable for CO_2 electro-conversion were placed in the flat-plate BESs (Reactor 1 and 2) and connected to a potentiostat (poised at −0.8 V vs. SHE). Both reactors were considered duplicates, since the operational conditions were identical but were operated during 175 days under different operation strategies in each batch (Table 1). The first two batches (1 and 2) were considered period under a high selection pressure due to the new electrochemical conditions (Fig. 4). Reducing power was provided directly by the electrode in form of electrons and/or H_2, and pure CO_2 (99.9% v/v) was used as the only carbon source. Adaptation period lasted around 40 and 30 days in reactors 1 and 2, respectively. Initially consumption of organic compounds was observed. Ethanol peaks (170 and 97 mM C) identified the first days in both reactors could be explained by the fermentation of remaining caproate or due to a

contamination during the manipulations of the cells (ethanol was used to maintain axenic conditions). After adaptation phase, both reactors started to produce acetate until the end of the first batch, once the pH was stabilized between 5.5 and 4. In this phase, current signal increased to 1.4 and 1.1 A m^{-2} $_{electrode}$ and more reducing equivalents were available. Until day 58, each system produced a maximum concentration of 64.80 and 42.52 mM C of acetate with productivities of 3.85 ± 2.51 and 2.17 ± 1.64 g m^{-2} $_{electrode}$ d^{-1} (Table 2), respectively. Accumulation of organics resulted on pH decreased (< 4 in the reactor 2) which might had triggered an episode of acid crash and subsequently the production stopped. CEs averaged 58% in reactor 1% and 57% in reactor 2 (Table 2).

A new batch (batch 2, day 30) was then started simultaneously in both systems by replacing 150 mL of catholyte with fresh medium. The anode medium was replaced with 150 mL of new fresh medium adjusted to a pH of 2 in order to maintain a high concentration of protons in the anodic chamber since the beginning of the subsequent new batch. In case of batch 3 onwards, both anolyte and catholyte were entirely replaced. During the second batch, the availability of nutrients, low pH
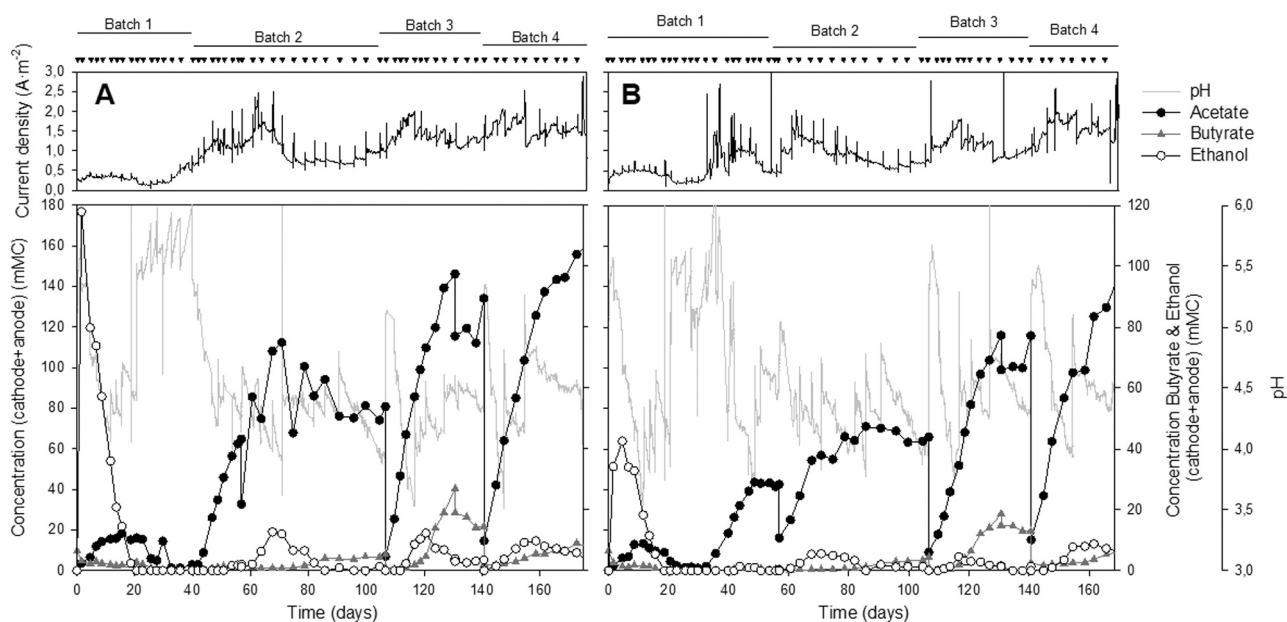

Fig. 4. Evolution of current signal, pH and total concentration of acetate, butyrate and ethanol over time in Reactor 1 (A) and Reactor 2 (B). Black inverted triangles on the top part of the figure indicate sampling and subsequent flushing with CO_2.

Table 2
Production rates of reactors 1 and 2 along the experiment.

Batch	Reactor 1 (R1) Production rates (g m^{-2}$_{electrode}$ d^{-1})					Reactor 2 (R2) Production rates (g m^{-2}$_{electrode}$ d^{-1})				
	Acetate	Ethanol	Butyrate	CE (%)	J (A m^{-2})	Acetate	Ethanol	Butyrate	CE (%)	J (A m^{-2})
1	3.85 ± 2.51	0.08 ± 0.17	0.08 ± 0.07	58 ± 41	0.54 ± 0.46	2.17 ± 1.64	0.04 ± 0.04	0.09 ± 0.22	57 ± 26	0.56 ± 0.48
2	7.04 ± 6.11	0.59 ± 0.67	0.21 ± 0.14	29 ± 22	1.00 ± 0.38	2.66 ± 1.88	0.10 ± 0.14	0.31 ± 0.27	27 ± 23	0.91 ± 0.31
3	7.46 ± 3.87	0.65 ± 0.71	0.99 ± 0.94	89 ± 35	1.38 ± 0.23	5.50 ± 2.71	0.83 ± 0.50	0.36 ± 0.38	21 ± 26	1.13 ± 0.30
4	5.15 ± 3.20	0.54 ± 0.31	0.25 ± 0.18	59 ± 34	1.56 ± 0.22	5.92 ± 4.00	0.17 ± 0.12	0.43 ± 0.51	28 ± 28	1.86 ± 0.72

(below 4.5) and the increasing current density (2 and 1.6 A m^{-2}, in reactor 1 and 2, respectively) leaded to a concomitant production of 7.04 ± 6.11 g$_{acetate}$ m^{-2}$_{electrode}$ d^{-1} and 0.59 ± 0.67 g$_{ethanol}$ m^{-2}$_{electrode}$ d^{-1}) in reactor 1.

Once the new feeding strategy was implemented, the third batch showed the highest productions rates of acetate in reactor 1 (7.46 ± 3.87 g m^{-2}$_{electrode}$ d^{-1}). Moreover, the production of ethanol triggered chain elongation of acetate towards butyrate in both reactors. Butyrate maximum concentrations reached 27 and 19 mM C with average production rates of 0.99 ± 0.94 and 0.36 ± 0.38 g m^{-2}$_{electrode}$ d^{-1} in reactors 1 and 2, respectively. Ethanol reached concentrations of 12 and 5 mM C with average production rates of 0.65 ± 0.71 and 0.83 ± 0.50 g m^{-2}$_{electrode}$ d^{-1}. In this batch, CEs increased to 89 ± 35% in reactor 1 and decreased to 21 ± 26% in reactor 2. The low CE in reactor 2, also seen in following batches, might be explained by the oxygen evolution reaction since oxygen produced in the anodic chamber migrates through the membrane or could be introduced during the sampling. During batch 2, small amounts of propionate, valerate and caproate were detected (data not shown) in both reactors, although not higher than 5 mM C in any case.

In batch 4 ethanol was also produced concomitantly with acetate in both reactors. Production rates increased from 5.50 to 5.92 g acetate m^{-2}$_{electrode}$ d^{-1}, 0.83–0.17 g ethanol m^{-2}$_{electrode}$ d^{-1} and from 0.36 to 0.43 g butyrate m^{-2}$_{electrode}$ d^{-1}.

As mentioned above, the increase in the current density leaded to the presence of more reducing equivalents in the medium, mainly in the form of H$_2$, which permitted reactions (e.g. ethanol production) that required more energy to be thermodynamically favorable [13,38].

New feeding strategy was conceived to favor the production of ethanol and more reduced compounds and was based on maintaining the reducing power and not fully saturate the catholyte with CO$_2$. This strategy was implemented after batch 2 and resulted in better product selectivity. In addition, feeding rate frequency was lowered and switched from 3 to 2 times per week, which decreased the partial pressure of CO$_2$ (pCO$_2$) between feeding points, which had been pointed out as an strategy to trigger chain elongation [9]. Continuous monitoring of the pH and the dissolved CO$_2$ in the liquid allowed to make decision accordingly to favor ethanol production, which would lead to an increase of the ethanol-to-acetate ratio triggering chain elongation-based reactions. However, the lack of continuous ethanol production obstructed this objective and therefore, butyrate productions were detected for short periods of time along the experiment. CO$_2$ was consumed at the beginning of each feeding event (Fig. S6 and Fig. S7) which ensures its biological utilization under the working conditions.

The fact that current signal was slightly different in each system explained the differences in production rates. Reactor 1 showed higher current signal than reactor 2 throughout the experiment. Interestingly, the current signal profile in both reactors followed the same trend described in the literature during concomitant production of acetate and ethanol during bio-electro CO$_2$ recycling (Fig. S6 and Fig. S7) [13].

Nevertheless, both systems showed acceptable resilience to operational changes and unexpected situations (e.g. power cuts, medium emptying, oxygen intrusion, run out of carbon source, etc.). In fact, the expected microbial lag phases at the beginning of batch 2, 3 and 4 were non-existing. This is surprising due to the lack of nutrients and high concentration of inhibitory compounds accumulated at the end of the previous batches. In this case, organics production started right after fresh medium was added and reached maximum production rates of 18 and 12 g m^{-2}$_{electrode}$ d^{-1} of products at different points of the experiment.

The new feeding strategy (implemented from batch 3 to the end of the experiment) favored the production of butyrate. This could be explained because the favorable conditions for ethanol production (low pH and high pH$_2$) were reached since the beginning, and ethanol was concomitantly produced and employed to trigger chain elongation through reverse β-oxidation for butyrate production (Fig. S8).

The effect of feeding CO_2 on the pH was not assessed in detail, although the values were described as optimal for triggering solventogenesis up to the literature [13]. pH_2 was clearly the parameter most influenced by the new strategy. Reducing equivalents were available since the beginning of each feeding event, contrary to the conventional CO_2 feeding procedure based to direct sparging in the liquid.

The lack of a continuous ethanol production, despite of the favorable operational parameters, might be explained by the low current density reached in both systems (< 2 A m^{-2}). This parameter had been already pointed out as crucial to trigger chain elongation by other authors, who also claimed H_2 reducing power is not enough to trigger solventogenesis on its own [9]. In fact, a clear increase of the current density was shown in both BESs (Fig. 4) due to (i) the biocathodic biofilm growth and (ii) the selection pressure towards electroactive species. These events suggested that more reduced compounds were likely to be obtained with this reactor in a long-term operation.

However, low pH values required to trigger ethanol productions were not reached due to pH gradients present in the biocathode. This low pH conditions could have also compromised the acetate production rate, since it dramatically decreased when pH was below 5 [39]. Kang and co-workers measured a persistent alkalinity in the proximity of the electrode during CO_2 electroreduction [40], which was where the electroactive biofilm habits and therefore the most affected by this phenomenon. However, ethanol production prevailed over butyrate production in reactor 1 when pH was lower than 4.3. When pH value increased, chain elongation was clearly triggered at batch (batch 4 –R1– and batch 3 –R2–; Fig. 4), which is in line of the stated by other authors [41,42].

3.4. Implications

The tested strategies should be considered as one step forward towards the implementation of a new full-scale technology to transform CO_2 into commodity chemicals. Novel studies on CO_2 feeding or how to enhance the settlement of electroactive microbes on the electrode are scarce. Even though those parameters were referred as crucial in the literature. An efficient way to provide the carbon source to the community is required to both maintain the biological activity and ensure full substrate availability during the CO_2 electro conversion.

Other approaches to improve the CO_2 feeding were focused on (i) using novel gas diffusion electrodes [43], (ii) changing CO_2 flow rates to overcome mass transfer limitations [15], (iii) add the CO_2 in the form of bicarbonate [44] and (iv) improving reactor geometries [45,46].

In the case of this study, the main novelty relies on the development of a new method to avoid the loss of reducing power in the system rather than a more sophisticated and effective way to feed CO_2. Thereby, highlighting the need of a facile methodology. Nevertheless, more research is needed to focus on how to operate better BES reactors and optimize them not only from the engineering, but also from the biological point of view.

4. Conclusion

This study established the basis of a new methodology to promote electroactive biofilm formation on the surface of an electrode prior to its connection to a power source. A previous fermentation adapted a community which was attached on the surface of carbon cloth that further acted as electrode during bio-electro CO_2 recycling process. The presence in the biofilm formed of the electroactive microorganism I-19 after the fermentation and subsequent autotrophic conditions was demonstrated. In addition, the community analysis revealed a compartmentalization of the system. The biofilm community not only differs from the planktonic one, but also between different points along the growth electrode surface. This suggested the existence of a substrate gradient that underlies the concomitant occurrence of different metabolic pathways during the fermentation process.

This pre-enriched biofilm was able to produce acetate, butyrate and ethanol during the bio-electro CO_2 recycling in two flat-plate BESs for over 270 and 170 days, respectively. Furthermore, a new feeding strategy was implemented which consisted of maintaining higher availability of reducing power since the beginning of the CO_2 feeding. Acetate was the main compound produced, whereas butyrate and ethanol were produced intermittently when the new feeding strategy was implemented. Nevertheless, both systems showed high resilience and robustness to operational changes and disturbances.

CRediT authorship contribution statement

R. Blasco-Gómez: Conceptualization, Data curation, Methodology, Investigation, Writing - Original Draft. **M. Romans-Casas:** Investigation, Data curation, Writing - Review & Editing. **S. Bolognesi:** Investigation, Writing - review & editing. **E. Perona-Vico:** Data curation, Writing - review & editing. **J. Colprim:** Writing - review & editing, Funding acquisition. **L. Bañeras:** Conceptualization, Methodology, Supervision, Writing - review & editing; **M. D. Balaguer:** Conceptualization, Methodology, Supervision, Writing - review & editing. **S. Puig**: Conceptualization, Methodology, Supervision, Funding acquisition, Writing - review & editing.

Declaration of Competing Interest

The authors declare that they have no known competing financial interests or personal relationships that could have appeared to influence the work reported in this paper.

Appendix A. Supporting information

Supplementary data associated with this article can be found in the online version at doi:10.1016/j.jece.2021.105549.

References

[1] K. Rabaey, R.A. Rozendal, Microbial electrosynthesis - revisiting the electrical route for microbial production, Nat. Rev. Microbiol. 8 (2010) 706–716.

[2] K.P. Nevin, T.L. Woodard, A.E. Franks, Z.M. Summers, D.R. Lovley, Meeting the challenge of developing and maintaining radical hysterectomy skills, BJOG Int. J. Obstet. Gynaecol. 117 (2010) 1–4, https://doi.org/10.1128/mBio.00103-10.

[3] R. Ganigué, S. Puig, P. Batlle-Vilanova, M.D. Balaguer, J. Colprim, Microbial electrosynthesis of butyrate from carbon dioxide, Chem. Commun. (Camb.) 51 (2015) 3235–3238.

[4] E.V. LaBelle, H.D. May, Energy efficiency and productivity enhancement of microbial electrosynthesis of acetate, Front. Microbiol. 8 (2017) 1–9.

[5] P. Batlle-Vilanova, R. Ganigue, S. Ramió-Pujol, L. Bañeras, G. Jiménez, M. Hidalgo, M.D. Balaguer, J. Colprim, S. Puig, Microbial electrosynthesis of butyrate from carbon dioxide: production and extraction, Bioelectrochemistry 117 (2017) 57–64.

[6] J.B.A. Arends, S.A. Patil, H. Roume, K. Rabaey, Phenotype, disease severity and pain are major determinants of quality of life in Fabry disease: results from a large multicenter cohort study, J. Inherit. Metab. Dis. 41 (2018) 141–149, https://doi.org/10.1016/j.jcou.2017.04.014.

[7] L. Jourdin, S.M.T. Raes, C.J.N. Buisman, D.P.B.T.B. Strik, Critical biofilm growth throughout unmodified carbon felts allows continuous bioelectrochemical chain elongation from CO_2 up to caproate at high current density, Front. Energy Res. 6 (2018) 7.

[8] I. Vassilev, P.A. Hernandez, P. Batlle-Vilanova, S. Freguia, J.O. Krömer, J. Keller, P. Ledezma, B. Virdis, Microbial electrosynthesis of isobutyric, butyric, caproic acids, and corresponding alcohols from carbon dioxide, ACS Sustain. Chem. Eng. 6 (2018) 8485–8493.

[9] L. Jourdin, M. Winkelhorst, B. Rawls, C.J.N. Buisman, D.P.B.T.B. Strik, Enhanced selectivity to butyrate and caproate above acetate in continuous bioelectrochemical chain elongation from CO_2: steering with CO_2 loading rate and hydraulic retention time, Bioresour. Technol. Rep. 7 (2019), 100284.

[10] I. Vassilev, F. Kracke, S. Freguia, J. Keller, J.O. Krömer, P. Ledezma, B. Virdis, Microbial electrosynthesis system with dual biocathode arrangement for simultaneous acetogenesis, solventogenesis and carbon chain elongation, Chem. Commun. (Camb.) 55 (2019) 4351–4354.

[11] A. Prévoteau, J.M. Carvajal-Arroyo, R. Ganigué, K. Rabaey, Microbial electrosynthesis from CO_2: forever a promise? Curr. Opin. Biotechnol. 62 (2020) 48–57.

[12] X. Christodoulou, T. Okoroafor, S. Parry, S.B. Velasquez-Orta, The use of carbon dioxide in microbial electrosynthesis: advancements, sustainability and economic feasibility, J. CO2 Util. 18 (2017) 390–399.

[13] R. Blasco-Gómez, S. Ramió-Pujol, L. Bañeras, J. Colprim, M.D. Balaguer, S. Puig, Unravelling the factors that influence the bio-electrorecycling of carbon dioxide towards biofuels, Green. Chem. 21 (2019) 684–691.

[14] R. Mateos, A. Sotres, R.M. Alonso, A. Morán, A. Escapa, Enhanced CO_2 conversion to acetate through microbial electrosynthesis (MES) by continuous headspace gas recirculation, Energies 12 (2019) 3297.

[15] M. del, P.A. Rojas, M. Zaiat, E.R. González, H. De Wever, D. Pant, Enhancing the gas–liquid mass transfer during microbial electrosynthesis by the variation of CO_2 flow rate, Process Biochem. 101 (2021) 50–58.

[16] B. Bian, S. Bajracharya, J. Xu, D. Pant, P.E. Saikaly, Microbial electrosynthesis from CO_2: challenges, opportunities and perspectives in the context of circular bioeconomy, Bioresour. Technol. 302 (2020), 122863.

[17] N. Cheng, Q. Liu, J. Tian, Y. Xue, A.M. Asiri, H. Jiang, Y. Hee, X. Suna, Acidically oxidized carbon cloth: a novel metal-free oxygen evolution electrode with high catalytic activity, Chem. Commun. (Camb.) 51 (2015) 1616–1619.

[18] S. Ramió-Pujol, University of Girona, 2016.

[19] S.A. Patil, S. Gildemyn, D. Pant, K. Zengler, B.E. Logan, K. Rabaey, A logical data representation framework for electricity-driven bioproduction processes, Biotechnol. Adv. 33 (2015) 736–744.

[20] M. Llirós, E.O. Casamayor, C. Borrego, High archaeal richness in the water column of a freshwater sulfurous karstic lake along an interannual study, FEMS Microbiol. Ecol. 66 (2008) 331–342.

[21] J.J. Kozich, S.L. Westcott, N.T. Baxter, S.K. Highlander, P.D. Schloss, Development of a dual-index sequencing strategy and curation pipeline for analyzing amplicon sequence data on the MiSeq Illumina sequencing platform, Appl. Environ. Microbiol. 79 (2013) 5112–5120.

[22] T. Stoeck, D. Bass, M. Nebel, R. Christen, M.D.M. Jones, H.W. Breiner, T. A. Richards, Multiple marker parallel tag environmental DNA sequencing reveals a highly complex eukaryotic community in marine anoxic water, Mol. Ecol. 19 Suppl 1 (2010) 21–31.

[23] R.C. Edgar, H. Flyvbjerg, Error filtering, pair assembly and error correction for next-generation sequencing reads, Bioinformatics 31 (2015) 3476–3482.

[24] R.C. Edgar, Search and clustering orders of magnitude faster than BLAST, Bioinformatics 26 (2010) 2460–2461.

[25] J.G. Caporaso, K. Bittinger, F.D. Bushman, T.Z. Desantis, G.L. Andersen, R. Knight, PyNAST: a flexible tool for aligning sequences to a template alignment, Bioinformatics 26 (2010) 266–267.

[26] S. Ramió-Pujol, R. Ganigué, L. Bañeras, J. Colprim, Incubation at 25 °C prevents acid crash and enhances alcohol production in Clostridium carboxidivorans P7, Bioresour. Technol. 192 (2015) 296–303.

[27] C.W. Marshall, E.V. LaBelle, H.D. May, Production of fuels and chemicals from waste by microbiomes, Curr. Opin. Biotechnol. 24 (2013) 391–397.

[28] X. Zhu, Y. Tao, C. Liang, X. Li, N. Wei, W. Zhang, Y. Zhou, Y. Yang, T. Bo, Molecular spectrum of KRAS, NRAS, BRAF and PIK3CA mutations in Chinese colorectal

cancer patients: analysis of 1,110 cases, Sci. Rep. 5 (2015) 18678, https://doi.org/10.1038/srep14360.

[29] M.V. Reddy, A. ElMekawy, D. Pant, Bioelectrochemical synthesis of caproate through chain elongation as a complementary technology to anaerobic digestion: bioelectrochemical chain elongation for higher carbon chemicals, Biofuels Bioprod. Bioref. 12 (2018) 966–977.

[30] D. Keogh, L.N. Lam, L.E. Doyle, A. Matysik, S. Pavagadhi, S. Umashankar, P. M. Low, J.L. Dale, Y. Song, S.P. Ng, C.B. Boothroyd, G.M. Dunny, S. Swarup, R.B. H. Williams, E. Marsili, K.A. Kline, Peer support and food security in deaf college students, J. Am. Coll. Health. J. ACH 68 (2020) 1–5, https://doi.org/10.1128/mBio.00626-17.

[31] E.M. Bosire, M.A. Rosenbaum, Electrochemical potential influences phenazine production, electron transfer and consequently electric current generation by pseudomonas aeruginosa, Front. Microbiol. 8 (2017) 1–11.

[32] L. Jourdin, S. Freguia, B.C. Donose, J. Keller, Autotrophic hydrogen-producing biofilm growth sustained by a cathode as the sole electron and energy source, Bioelectrochemistry 102 (2015) 56–63.

[33] R. Mateos, A. Sotres, R.M. Alonso, A. Escapa, A. Morán, Impact of the start-up process on the microbial communities in biocathodes for electrosynthesis, Bioelectrochemistry 121 (2018) 27–37.

[34] A. Cournet, M.L. Délia, A. Bergel, C. Roques, M. Bergé, Electrochemical reduction of oxygen catalyzed by a wide range of bacteria including Gram-positive, Electrochem. Commun. 12 (2010) 505–508.

[35] C.W. Marshall, D.E. Ross, K.M. Handley, P.B. Weisenhorn, J.N. Edirisinghe, C. S. Henry, J.A. Gilbert, H.D. May, R.S. Norman, Metabolic reconstruction and modeling microbial electrosynthesis, Sci. Rep. 7 (2017) 8391.

[36] E. Yabuuchi, Y. Kosako, H. Oyaizu, I. Yano, H. Hotta, Y. Hashimoto, T. Ezaki, M. Arakawa, Proposal of Burkholderia gen. nov. and transfer of seven species of the genus Pseudomonas homology group II to the new genus, with the type species Burkholderia cepacia (Palleroni and Holmes 1981) comb. nov, Microbiol. Immunol. 36 (1992) 1251–1275.

[37] M. Zhou, S. Freguia, P.G. Dennis, J. Keller, K. Rabaey, Development of bioelectrocatalytic activity stimulates mixed-culture reduction of glycerol in a bioelectrochemical system, Microb. Biotechnol. 8 (2015) 483–489.

[38] S.M.T. Raes, L. Jourdin, C.J.N. Buisman, D. Strik, Continuous long-term bioelectrochemical chain elongation to butyrate, ChemElectroChem 4 (2017) 386–395.

[39] E.V. LaBelle, C.W. Marshall, J.A. Gilbert, H.D. May, Influence of acidic ph on hydrogen and acetate production by an electrosynthetic microbiome, PLoS One 9 (2014), e109935.

[40] K. Yang, R. Kas, W.A. Smith, In situ infrared spectroscopy reveals persistent alkalinity near electrode surfaces during CO_2 electroreduction, J. Am. Chem. Soc. 141 (2019) 15891–15900.

[41] K.J.J. Steinbusch, H.V.M. Hamelers, C.M. Plugge, C.J.N. Buisman, Biological formation of caproate and caprylate from acetate: fuel and chemical production from low grade biomass, Energy Environ. Sci. 4 (2011) 216–224.

[42] T.I.M. Grootscholten, K.J.J. Steinbusch, H.V.M. Hamelers, C.J.N. Buisman, Chain elongation of acetate and ethanol in an upflow anaerobic filter for high rate MCFA production, Bioresour. Technol. 135 (2013) 440–445.

[43] S. Bajracharya, K. Vanbroekhoven, C.J.N. Buisman, D. Pant, D.P.B.T.B. Strik, Application of gas diffusion biocathode in microbial electrosynthesis from carbon dioxide, Environ. Sci. Pollut. Res. Int. 23 (2016) 22292–22308.

[44] G. Mohanakrishna, I.M. Abu Reesh, K. Vanbroekhoven, D. Pant, Microbial electrosynthesis feasibility evaluation at high bicarbonate concentrations with enriched homoacetogenic biocathode, Sci. Total Environ. 715 (2020), 137003.

[45] T. Krieg, J. Madjarov, L.F. M. Rosa, F. Enzmann, F. Harnisch, D. Holtmann and K. Rabaey, Adv. Biochem. Eng. Biotechnol., DOI:⟨10.1007/10_2017_40⟩.

[46] F. Enzmann, F. Mayer, M. Stöckl, K.M. Mangold, R. Hommel, D. Holtmann, Transferring bioelectrochemical processes from H-cells to a scalable bubble column reactor, Chem. Eng. Sci. 193 (2019) 133–143.